Master of Science

Correlation of phospholipidosis between mouse liver three dimensional (3D) organoids and *in vivo* mouse

The Graduate School
of the University of Ulsan

Department of Medicine
Sang-Joon Lee

Correlation of phospholipidosis between mouse liver three dimensional (3D) organoids and *in vivo* mouse

Supervisor : Woo-Chan Son

A Dissertation

Submitted to
the Graduate School of the University of Ulsan.
In partial Fulfillment of the Requirements
for the Degree of

Master of Science

by

Sang-Joon Lee

The Graduate School
of the University of Ulsan

Department of Medicine
December 2018

Correlation of phospholipidosis between mouse liver three dimensional (3D) organoids and *in vivo* mouse

This certifies that the master's thesis

of Sang-Joon Lee is approved.

_____

Committee Chair Dr. Hyeong-Seok Lim

_____

Committee Member Dr. Heon-sik Choi

_____

Committee Member Dr. Woo-Chan Son

The Graduate School of the University of Ulsan

Department of Medicine

December 2018

List of abbreviations

3D;	Three dimensional
ALB;	Albumin
AMD;	Amiodarone
AP1S1;	Adaptor-related protein complex 1, sigma 1 subunit
APAP;	Acetaminophen
ASAH1;	N-acylsphingosine amidohydrolase (acid ceramidase)1
DILI;	Drug-induced liver injury
DIPL;	Drug-induced phospholipidosis
DM;	Differentiation medium
EM;	Expansion medium
H&E;	Hematoxylin and Eosin
IHC;	Immunohistochemistry
KRT19;	Keratin 19
LAMP2;	Lysosome-associated membrane protein 2
LGR5;	leucine-rich repeat-containing G protein-coupled receptor 5
SOX9;	SRY-box 9
TDZ;	Thioridazine
TEM;	Transmission electron microscopy
TMX;	Tamoxifen

Abstract

The purpose of this study was to test whether the phenomena of phospholipidosis in mouse liver organoids was identical with that in *in vivo* mouse toxicity studies. For this purpose, the organoids were differentiated from liver stem cells of a C57BL/6 mouse and three compounds, amiodarone, tamoxifen and thioridazine, were treated to induce DIPL to the organoids for 72 hours. After differentiation, the organoids displayed compact spherical appearance composed of uniformly polygonal cells. Furthermore, the organoids showed a notable lower expression of adult stem cell genes, whereas hepatic progenitor/biliary gene and early hepatocyte gene levels were higher than those of the liver stem cells. The electron microscopy examination showed the intracytoplasmic aggregations of the multilamellar bodies, a hallmark of DIPL, in amiodarone-treated organoids. And histological examination and gene expression associated with DIPL supported the result from electron microscopy. Our findings suggest that mouse liver organoids can reflect well the expected or well-known outcomes in phospholipidosis-induced *in vivo* mouse and can support further researches for predicting the DIPL in liver organoids.

Keywords: Phospholipidosis; Cationic amphiphilic drugs; Mouse liver organoid

Contents

List of Tables

List of Figures

Introduction

1. Drug-induced liver injury (DILI)

The liver is an essential organ for glycogen storage, control of metabolism, regulation of cholesterol synthesis and transport, urea metabolism, secretion of plasma proteins such as albumin, and drug detoxification (Si-Tayeb, Lemaigre, & Duncan, 2010). This organ is especially susceptible to toxic agents because it is usually the first place for drugs to pass through and drugs can cause a hepatotoxicity through metabolism, one of the main functions of the liver.

Drug-induced liver injury (DILI) is a broad term applied to any injury of liver caused by drugs from asymptomatic liver diseases to acute liver failure. DILI may be the result of direct toxicity from the administered drug or their metabolites, or inflammation. Drugs are usually metabolized by the cytochromes P450 (CYPs) in a series of phase I and phase II reactions. Toxic intermediates can cause hepatocellular damage and death by inducing apoptosis or necrosis. Drugs that bind to cellular membranes can induce an immunologic reaction by presentation to major histocompatibility complex (MHC) particles, resulting in inflammation (**Figure 1**) (David & Hamilton, 2010).

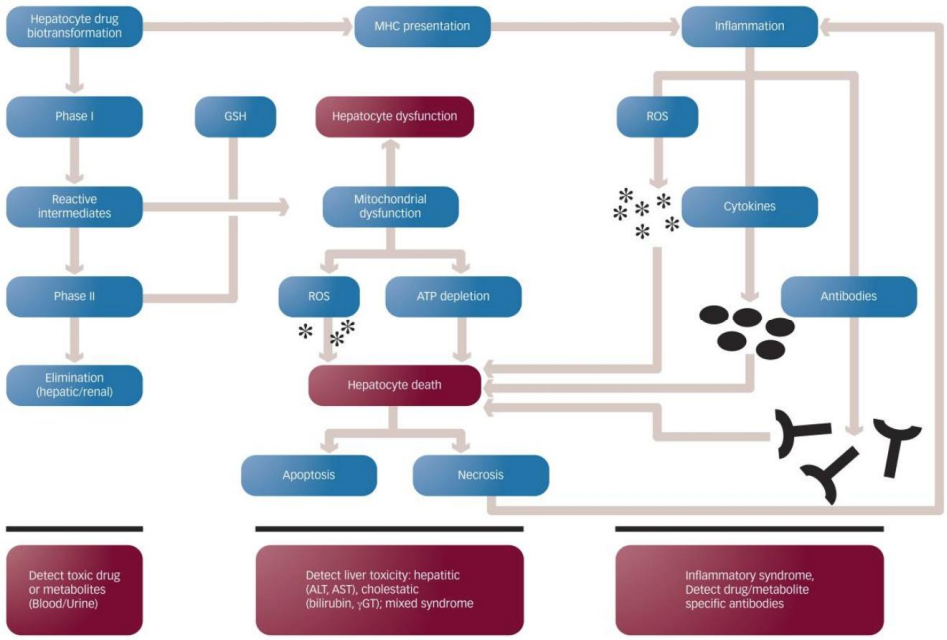

Figure 1. Mechanisms of Drug-Induced Liver Injury. Cited from David, Stefan, and James P. Hamilton. "Drug-induced liver injury." *US gastroenterology & hepatology review* 6 (2010): 73.

DILI has been considered as a major reason for toxicological issues in drug development and one of the most frequent causes for drug withdrawals or restrictions (**Figure 2**) (Bell et al., 2017; Cherblanc, Chapman-Rothe, Brown, & Fuchter, 2012; Stevens & Baker, 2009). Of 76 drugs withdrawn from the market from 1969 to 2002, 12 drugs were attributable to liver damage. Whereas drugs that were not detected for DILI during drug approval result in post-marketing restrictions, the risk of false positive DILI may lead to unnecessary attrition, thereby contributing to the considerable economic issues associated with DILI. Recent examples include the attrition of fasiglifam, which was terminated only in phase III due to concerns about liver safety (Otieno et al., 2017), the termination of AZD1979 due to unexplained ALT elevations in the clinic, and the restricted-use warnings of flupirtine, pazopanib, and temozolomide due to signs of hepatotoxicity that remained unnoticed during clinical stage (Kullak-Ublick et al., 2017).

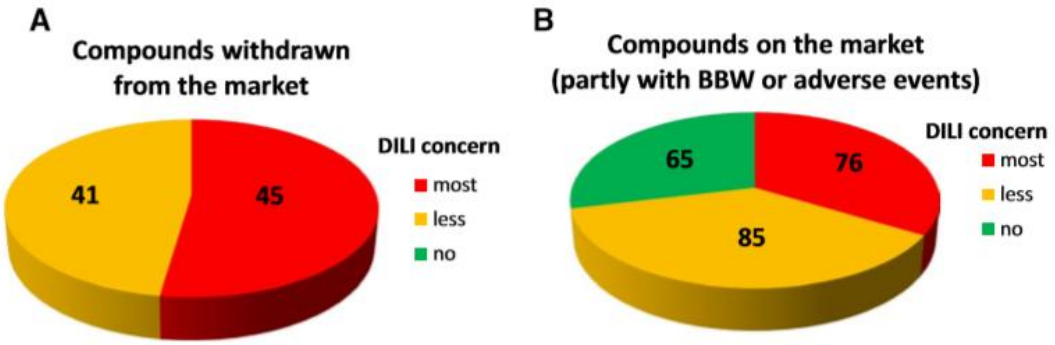

Figure 2. Extent of DILI concern in compounds withdrawn from the market or with black box warning, adverse events or no concern for DILI. Cited from Cherblanc, F., et al. "Current limitations and future opportunities for epigenetic therapies." *Future medicinal chemistry* 4.4 (2012): 425-446.

2. Drug-induced phospholipidosis (DIPL)

Drug-induced phospholipidosis (DIPL) is a lipid storage disorder in which phospholipid-drug complexes accumulate within lysosomes as lamellar inclusion bodies. Since a first noted condition was characterized by hepatosplenomegaly, foamy cells, and vacuolated peripheral lymphocytes (Kodavanti & Mehendale, 1990), DIPL is characterized as phospholipid accumulation in affected tissues of which lung, liver, brain, kidney, cornea and others by using transmission electron microscopy which is regarded as the 'gold standard' for diagnosis of DIPL (Anderson & Borlak, 2006; Nonoyama & Fukuda, 2008; Seydel & Wassermann, 1976). Cationic amphiphilic drugs (CADs) include antibiotics, antidepressants, antipsychotics, antimalarial and antiarrhythmic drugs. Many of these contain a hydrophilic ring and hydrophobic regions and have been reported to induce the DIPL in many tissues, commonly liver and lung (Anderson & Borlak, 2006; Chatman, Morton, Johnson, & Anway, 2009; Halliwell, 1997; Reasor, Hastings, & Ulrich, 2006). Amiodarone, an antiarrhythmic compound with a CAD structure, is the most representative compound that causes DIPL (Horn et al., 1996; Nioi, Perry, Wang, Gu, & Snyder, 2007).

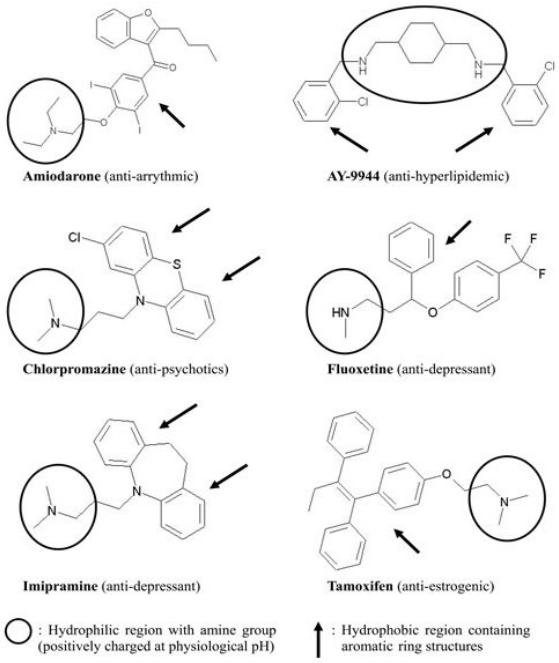

Figure 3. Chemical structures of representative cationic amphiphilic drugs. Cited from Nonoyama, Takashi, and Ryo Fukuda. "Drug-induced phospholipidosis-pathological aspects and its prediction." *Journal of toxicologic pathology* 21.1 (2008): 9-24.

The regulatory forum about DIPL presents a risk management strategy for selection and development of compounds with potential to produce DIPL (Chatman et al., 2009). The first tier uses *in silico* and *in vitro* assays to select compounds with reduced probability of producing DIPL. In the second tier, representative compounds with an acceptable combination of limited DIPL liabilities, desirable pharmaceutical properties, and evidence of efficacy are tested in exploratory *in vivo* studies to determine if the compounds cause DIPL and to develop structure-activity relationships. Fourteen-day studies in the rodent and nonrodent species are recommended to be used for GLP studies.

If a compound shows enough promise to develop despite evidence of DIPL in animals, a scientifically based risk management strategy incorporating standard nonclinical studies (including assessment of reversibility) and targeted clinical monitoring may be used to evaluate the human safety risks.

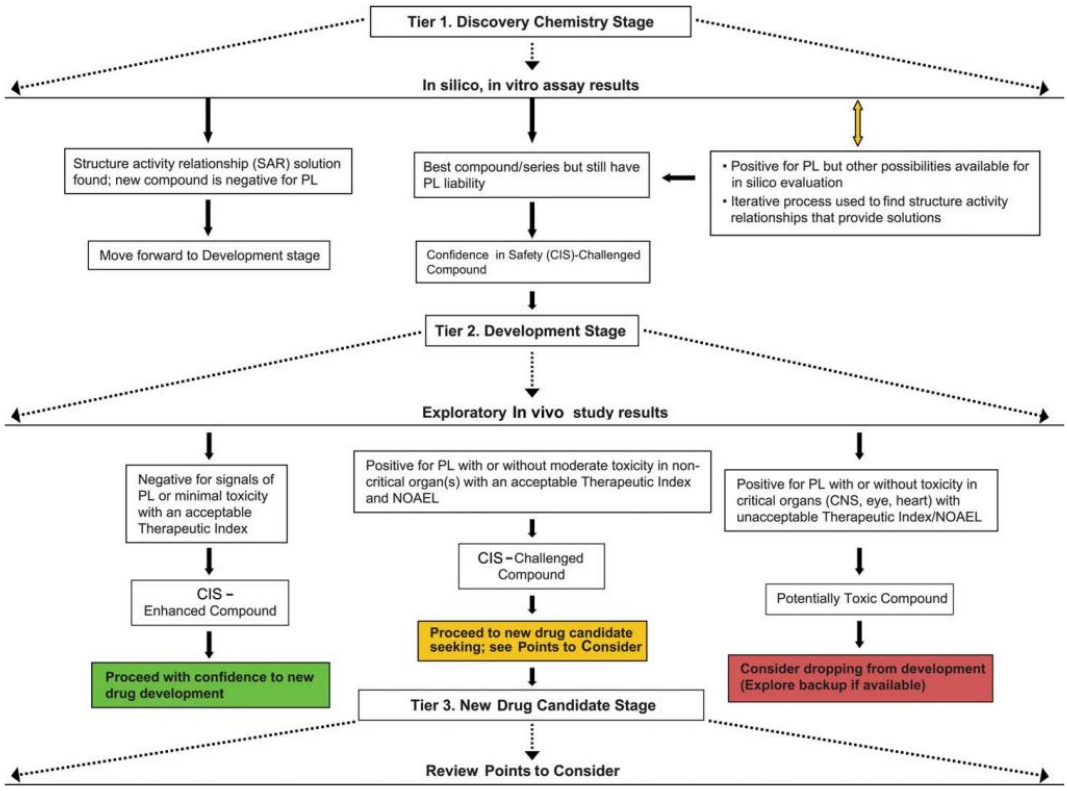

Figure 4. Tier strategy process. Chatman, Linda A., et al. "A strategy for risk management of drug-induced phospholipidosis." *Toxicologic pathology* 37.7 (2009): 997-1005.

It is recommended that the preclinical toxicity studies to identify the DIPL be conducted for two weeks in the rodent and non-rodent species (Chatman et al., 2009). However, the process is quite expensive and time-consuming to confirm the DIPL by using TEM. Therefore, it is recommended to easily and quickly identify and screen out those compounds with the potential to lead DIPL in early discovery stage.

3. Liver 3D organoid

Liver organoids are *in vitro* systems that culture primary hepatocytes or liver stem cells in three-dimension. These three-dimensional liver organoid culture systems have been studied actively. Recently, Clevers et al. developed for the mouse liver organoids and the human liver organoids which were differentiated from liver stem cells (Huch et al., 2013; Huch et al., 2015). They are known to have more physiologically relevant environment, cell-cell interactions and organ-like microarchitectures than those of conventional *in vitro* culture models such as two-dimensional models or sandwich culture models (Godoy et al., 2013; Schyschka et al., 2013; Takahashi et al., 2015). These advantages make the liver organoids to have an improved hepatocellular differentiation, *in vivo* like functionalities, and to well-preserved hepatocellular phenotypes during long-term cultivation (Bell et al., 2017). For these reasons, the liver organoids have been considered as useful models in the areas of early drug discovery and toxicology (Edmondson, Broglie, Adcock, & Yang, 2014). Importantly, recent studies have proved that the liver organoids can perform chronic toxicity studies and be suitable to study a variety of drug-induced liver injuries (DILIs) (Fatehullah, Tan, & Barker, 2016; Funk & Roth, 2017; Leite et al., 2012).

In this study, we hypothesized that liver organoids derived from C57BL/6 mouse liver tissue could perform *in vivo* phenomena of DIPL. After the characterization and differentiation of mouse liver organoids, we treat the amiodarone to the organoids and investigate whether the multilamellar bodies are observed in cytoplasm of the mouse liver organoids by using electron microscopy. To our knowledge, this is the first study that investigated the *in vitro* to *in vivo* extrapolation in DIPL by using mouse liver organoids.

Materials and Methods

1. Mouse liver organoids

C57BL/6 mouse were used for making the mouse liver organoids. Each medium composition was decided from the previous study (Broutier et al., 2016). Freshly isolated liver was stored at 4 ℃ in basal medium that is Advanced DMEM/F-12 (Life Technologies, cat. no. 12634-010) supplemented with 1% penicillin/streptomycin (Life Technologies, cat. no. 15140-122), 1% GlutaMAX (Life Technologies, cat. no. 35050-068) and HEPES 10 mM (Life Technologies, cat. no. 15630-056). The isolated liver tissue was chopped into roughly 0.5 mm^3 pieces at 100-mm Petri dish, and these tissue pieces were transferred to 15ml centrifuge tube. And after adding cold wash medium, the tissue pieces were centrifuged at 300g for 5min at 8 ℃. The resulting cell pellet was resuspended in ice-cold Matrigel (BD, cat. no. 356231) and plated as 50μl droplets of a warm 24 well plate. After the Matrigel had solidified, mouse isolation medium, consisting of the basal medium supplemented with 1:50 B27 supplement (Life Technologies, cat. no. 12587-010), 1 mM N-acetylcysteine (Sigma-Aldrich, cat. no. A0737-5MG), 5% (vol/vol) Rspo1-conditioned medium (Trevigen, cat. no. 3710-001-01), 10 mM nicotinamide (Sigma-Aldrich, cat. no. N0636), 10 nM recombinant human [Leu15]-gastrin I (Sigma-Aldrich, cat. no. G9145), 50 ng/ml recombinant mouse EGF (Life Technologies, cat. no. PMG8043), 100 ng/ml recombinant human FGF10 (Peprotech, cat. no. 100-26), 50 ng/ml recombinant human HGF (Peprotech, cat. no. 100-39), 25 ng/ml recombinant human Noggin (Peprotech, cat. no. 120-10C), 30% (vol/vol) Wnt3a-conditioned medium, and 10 μM Rho kinase (ROCK) inhibitor (Y-27632; Sigma-Aldrich, cat. no. Y0503), was added to each well. After 3 days, the isolation medium was replaced with mouse liver expansion medium lacking Wnt, Noggin, and Rock inhibitors. In this stage, 10^4 mouse liver stem cells were seeded.

Mouse liver stem cells or organoids were cultured in a humidified tissue culture incubator with 5% CO_2 and atmospheric O_2 at 37 °C. The expansion medium was refreshed every other day. For differentiation, the expansion medium was replaced with differentiation medium containing A83-01 (Tocris Bioscience, cat. no. 2939) and DAPT (Sigma-Aldrich, cat. no. D5942) and lacking RSPO1, HGF and nicotinamide. The differentiation medium was changed every other day for a period of 10 days.

2. *in vivo* mouse study

A total of 30 healthy, approximately 6-week-old, male C57BL/6 mouse were supplied by Orient Bio (Korea) and acclimatized for 2 weeks before the start of the experiment. Animals were group housed (3 mouse/cage) in polysulfone cages with a wire mesh roof under routine conditions of temperature, relative humidity, ventilation, and illumination. Rats were fed an autoclaved pellet diet *ad libitum* with free and continuous access to drinking water. Prior to blood sampling and euthanasia, animals had access to water and were fasted. The study protocol was reviewed and approved by the Animal Care and Use Committee of the Asan Medical Center (IACUC No. 2017-12-275).

3. Selection of compounds

Amiodarone (Sigma-Aldrich, cat. no. A8423), tamoxifen (Sigma-Aldrich, cat. no. T5648), thioridazine (Sigma-Aldrich, cat. no. T9025) and acetaminophen (Sigma-Aldrich, cat. no. A7085) were chosen by referring to the previous studies (Bhandari, Figueroa, Lawrence, & Gerhold, 2008; Somani, Bandyopadhyay, Klaunig, & Gross, 1990). Information on each drug can be found in **Table 1**.

Table 1. Background information on drug used in the current study

Compound	Induction of DIPL	References
Amiodarone	Yes	Honegger et al., 1993; Kasahara et al., 2006
Tamoxifen	Yes	Kasahara et al., 2006; Reasor and Kacew, 2001
Thioridazine	Yes	Kasahara et al., 2006; Lullmann-Rauch, 1974
Acetaminophen	No (Negative control)	Jaeschke et al., 2002; Waters et al., 2001

4. Study designs

4.1. Mouse liver organoid

The study design was depicted in **Figure 5**. Prior to the start of treatment, the expansion medium was replaced with the differentiation medium. And the differentiation medium was changed every other day for 14 days. After 14 days, organoids were treated with each compound (AMD; 10μM, TMX; 2.5, 10, and 20μM, TDZ; 2.5, 10, and 20μM, and APAP; 10μM) for 72 hours.

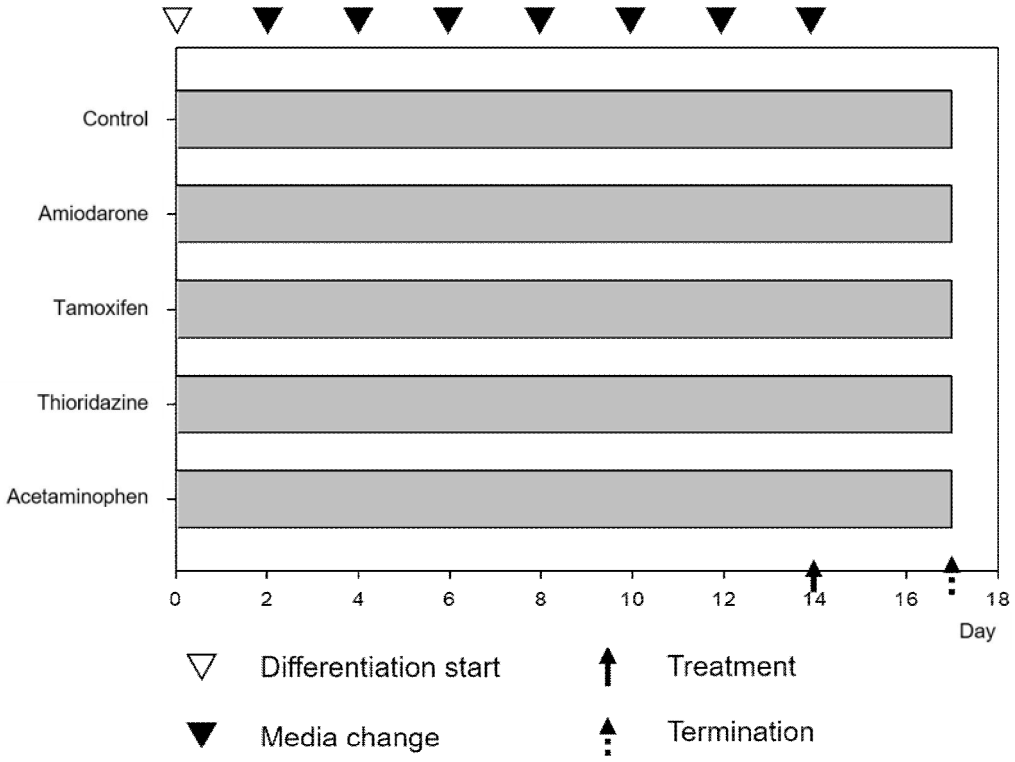

Figure 5. Study design for mouse liver organoid. After Mouse liver organoids were incubated with DM medium for 14 days, each compound (AMD; 10μM, TMX; 2.5, 10, and 20μM, TDZ; 2.5, 10, and 20μM, and APAP; 10μM) were treated for 72 hours.

4.2. *In vivo* mouse toxicity study

Prior to the start of treatment, animals were randomly allocated to the vehicle (one group of six mouse) or treatment groups (four groups of six mouse each). Mouse were treated with repeated dose of AMD (1000mg/kg orally; Sigma), APAP (1000mg/kg orally; Sigma), TMX (300mg/kg orally; Sigma), and TDZ (300mg/kg orally; Sigma) or vehicle (0.5% carboxy methylcellulose; Sigma) for 7 days. The level of each compound was set at the maximum tolerated dose based on clear signs of toxicity with little or no lethality (Bhandari et al., 2008; Somani et al., 1990). The injection volume for each treatment or vehicle was 10 mL/kg body weight. Clinical observations were performed daily, and body weight was recorded prior to dosing and euthanasia. Blood was collected from the caudal vena cava before necropsy.

Table 2. Study design for in vivo mouse toxicity study.

Group	Dose (mg/kg)	Route of administration	No. of Animal
Control	0	Oral	6
Amiodarone	1000	Oral	6
Acetaminophen	1000	Oral	6
Tamoxifen	300	Oral	6
Thioridazine	300	Oral	6

5. Serum biomarkers

Serum albumin, ALP, AST, and ALT levels were measured using an automated clinical chemistry analyzer (Hitachi 7180; Hitachi High-Technologies, Japan).

6. RNA isolation, cDNA synthesis and quantitative reverse transcription PCR

RNA from organoids cultured in the expansion medium and the differentiation medium was isolated and converted to cDNA as described previously (Nantasanti et al., 2015). QPCR was performed in duplicate on three culture replicates per donor on a BioRad MyiQ thermal cycler using SYBRgreen supermix (BioRad). Species specific primers were developed for albumin (ALB); SRY-box 9 (SOX9); and leucine-rich repeat-containing G protein-coupled receptor 5 (LGR5). SOX9 and LGR5 were used as adult stem cell genes, KRT19 was used as hepatic progenitor/biliary gene, and ALB was used as early hepatocyte gene (Huch et al., 2013). In addition, N-acylsphingosine amidohydrolase (acid ceramidase)1 (ASAH1) was used as phospholipidosis marker (Nioi et al., 2007). Sequence information can be found in **Table 3**.

Table 3. Primer sequences of KRT19, ALB, HNF4α, SOX9, LGR5, ASAH1, and AP1S1

Species	Gene	Direction	Sequence (5' – 3')
Mouse	KRT19	Forward	GGACCCTCCCGAGATTACAACCA
		Reverse	GCCAGCTCCTCCTTCAGGCTCT
	ALB	Forward	GCAGATGACAGGGCGGAACTTG
		Reverse	AAAATCAGCAGCAATGGCAGGC
	SOX9	Forward	TGCCCATGCCCGTGCGCGTCAA
		Reverse	CGCTCCGCCTCCTCCACGAAGGGTCT
	LGR5	Forward	AGGCTGCCAAAAACTTCAGA
		Reverse	TCCATGCTAAGTTCAGAGATCG
	ASAH1	Forward	TCCGTGGCACACCATAAATCT
		Reverse	TCCACTTGGCACAAATGTATTCA

7. Cell viability assay

Cell viability was assayed using the ATPlite 3D, 300 Assay Point Kit (PerkinElmer, cat. no. 6066943) to monitor relative levels of ATP by using the manufacturer's protocol. To confirm optimal doses of each compounds, ATP cell viability assay was conducted.

8. Pathology

8.1. *In vivo* mouse liver

Necropsy was performed on all animals, with macroscopic evaluation of the thoracic and abdominal cavity and tissues. After macroscopic examination, the excised liver was fixed in 10% neutral buffered formalin. Two lobes (the left lateral lobe and the median lobe) were sectioned and washed with tap water for approximately 6 h to remove formaldehyde. Tissues were then dehydrated in graded ethanol and cleared in xylene using an Excelsior S tissue processor (Thermo Scientific, USA), after which they were embedded in paraffin blocks using an EG1150H paraffin embedding station (Leica, Germany). The paraffin blocks were cut into 4 μm sections on an RM2255 rotary microtome (Leica). Sections were mounted onto glass slides, and hematoxylin and eosin staining and coverslipping were performed on an Autostainer XL (Leica). Histological examination of livers was performed by an experienced pathologist.

8.2. Mouse liver 3D organoid

The mouse liver organoids were fixed with 10% neutral buffered formaline for 30 min. After washing cells with phosphate-buffered saline (PBS) twice, cells were collected into 1.5 mL tube to spin down gently. Cell pellets were embedded with Histogel, specimen processing gel. Solidified gel was transferred to tissue cassettes and paraffin blocks were made by standard method. on an RM2255 rotary microtome (Leica). Sections were mounted onto glass slides, and hematoxylin and eosin staining and coverslipping were performed on an Autostainer XL (Leica). Histological examination of livers was performed by an experienced pathologist.

9. Immunohistochemistry

Sections from paraffin-embedded tissue blocks were cut at a 4 μm thickness and mounted on glass slides. Immunohistochemistry was carried out using a Benchmark XT (Ventana Medical Systems Inc., Tucson, AZ). Deparaffinization, epitope retrieval, and immunostaining were performed according to the manufacturer's instructions using cell conditioning solutions (CC1) and the BMK ultraView diaminobenzidine (DAB) detection system (Ventana Medical Systems). Slides were stained with anti-LAMP2 (Thermo Fisher, cat. no. PA1-655). Positive signals were amplified using ultraView copper, and sections were counterstained with hematoxylin and bluing reagent.

10. Electron microscopy

One 24-well plate per group was used when the organoids were about 70% ~ 80% per well in the 24-well plate. Organoids were immersion fixed in glutaraldehyde 3% in potassium phosphate buffer 0.09 M 1.4% sucrose. Samples were embedded and cut in semithin and ultrathin sections. For contrast, the ultrathin sections were incubated for 8 min on a drop of 0.5% uranyl acetate in Milli-Q, then rinsed thoroughly with Milli-Q, and further stained for 8 min on a drop of lead citrate in Milli-Q, rinsed again and dried before examination in a Philips CM100 electron microscope.

11. Statistical analysis

Data are expressed as the means ± SEM. Significance differences between the APAP-dosed and vehicle groups were assessed by ANOVA and Dunnett’s post hoc test using SPSS (IBM SPSS Statistics 23 Software, USA). Fold changes in biomarker expression levels are expressed versus the vehicle group. P values < 0.05 were considered statistically significant.

Results

1. Characterization of the mouse liver organoids

1.1. Morphology of the mouse liver organoids

After adding the mouse isolation medium to each well, about 200μm of ductal fragments were observed in the solidified Matrigel (**Figure 6A**). These duct cells expanded into the spherical shaped organoids when replacing the isolation media with the expansion medium (**Figure 6B**). They maintained relatively uniform size during the first few days. After media change into the differentiation medium, it was identified that the cells constituting the organoids were darkened and the shape of these cells had uniformly polygonal structure (**Figure 6C, D).**

Histologically, the mouse liver organoids in the expansion medium displayed a simple columnar epithelium with lumen (**Figure 7A)**. The uniformly polygonal cells were also observed in the organoids stained with hematoxylin and eosin (**Figure 7B**). When cultured in this differentiation medium, the lumen was still existed. However, duct-like cells acquired more hepatocellular morphologies, including round to oval nucleus, one nucleolus, and abundant cytoplasm. No significant apoptosis/necrosis was observed in these organoids.

1.2. Changes in stem cell, ductal and hepatocyte markers

Gene expressions of LGR5, the ducal markers, and SOX9, the stem cell marker, decreased in the mouse liver organoids cultured in the differentiation medium, while KRT19, the stem cell markers, and ALB, the hepatocyte markers, increased in the mouse liver organoids cultured in the differentiation medium. The mean LGR5 and SOX9 levels were 0.016-fold and 0.085-fold lower, respectively, than those of the organoids in the expansion medium (**Figure 8A, B**). And the mean KRT19 and ALB levels were 2.928-fold and 10.907-fold higher, respectively, than those of the organoids in the expansion medium (**Figure 8C, D**).

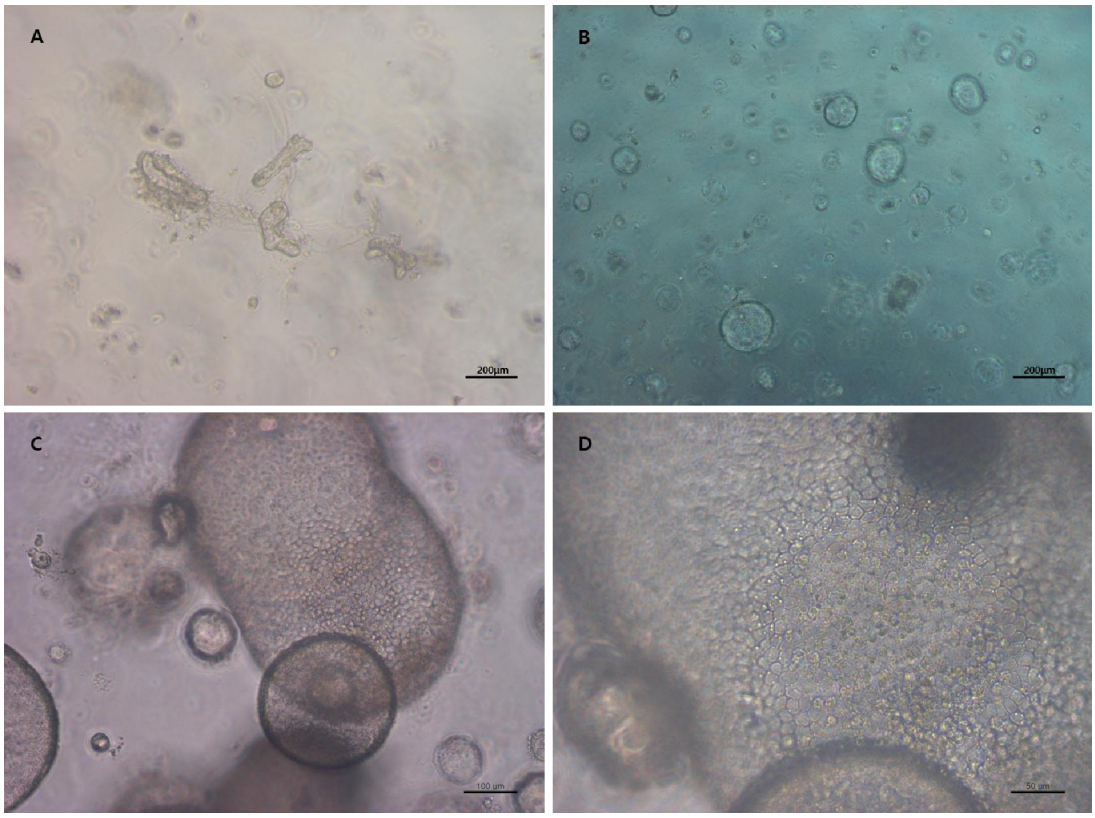

Figure 6. Representative inverted microscopic images of the mouse liver organoids at each stage. (A) Isolation stage. The ductal fragments obtained after chopping the mouse liver tissue. Scale bar = 200 μm. (B) Expansion stage. The isolated duct cells expanded into the spherical shaped organoids. Scale bar = 200 μm. (C) Differentiation stage. The mouse liver organoids (day 12) in the differentiation medium. The liver organoids differentiated into uniform polygonal structure. Scale bar = 100 μm. (D) Higher magnification of (C). Scale bar = 50 μm.

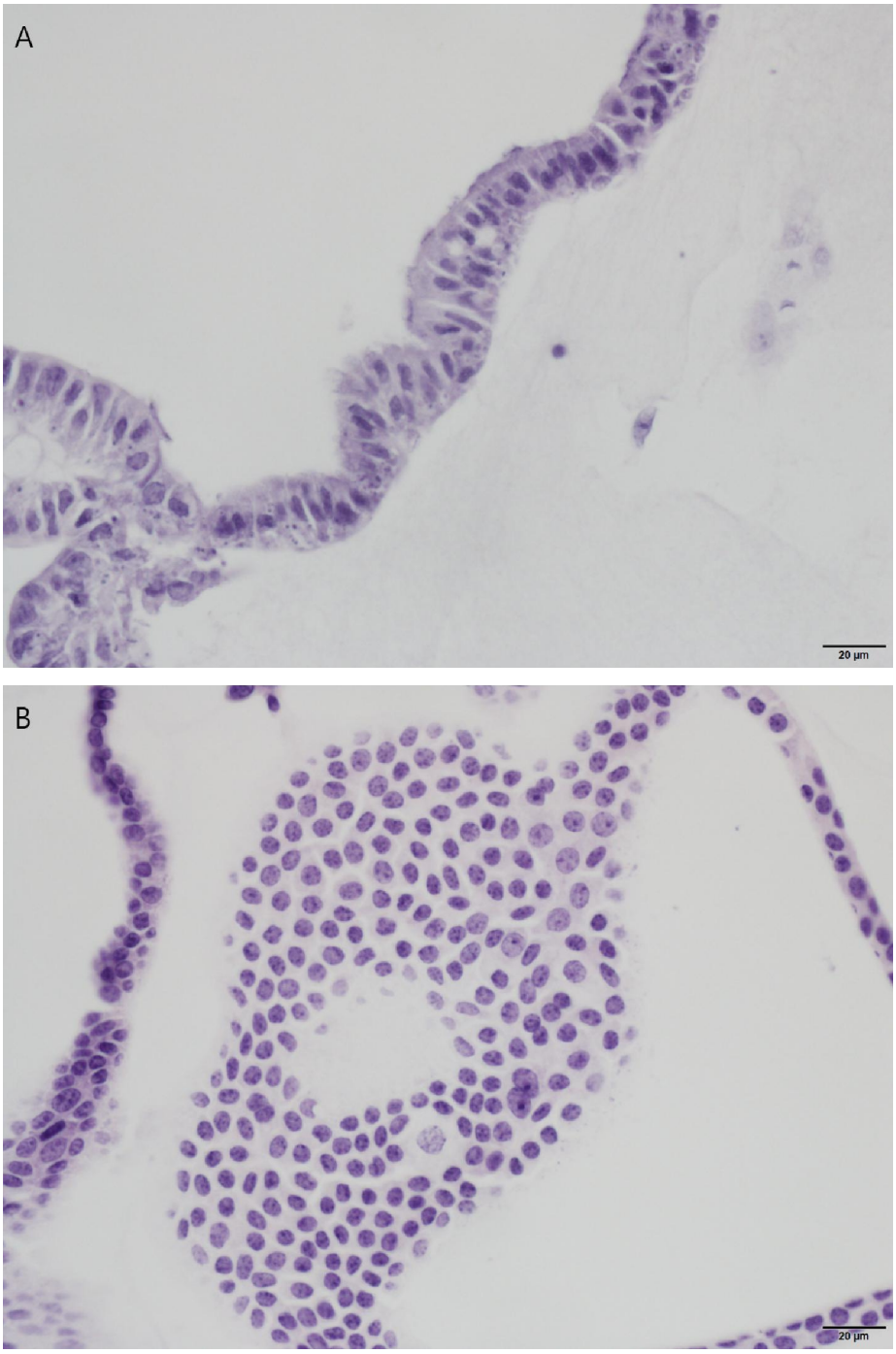

Figure 7. Representative histological images of the mouse liver organoids stained with hematoxylin and eosin. 400×. Scale bars = 20 μm. (A) Mouse liver organoid in expansion medium at day 14. Simple columnar epithelium with lumen were observed. (B) Mouse liver organoid in differentiation medium at day 14.

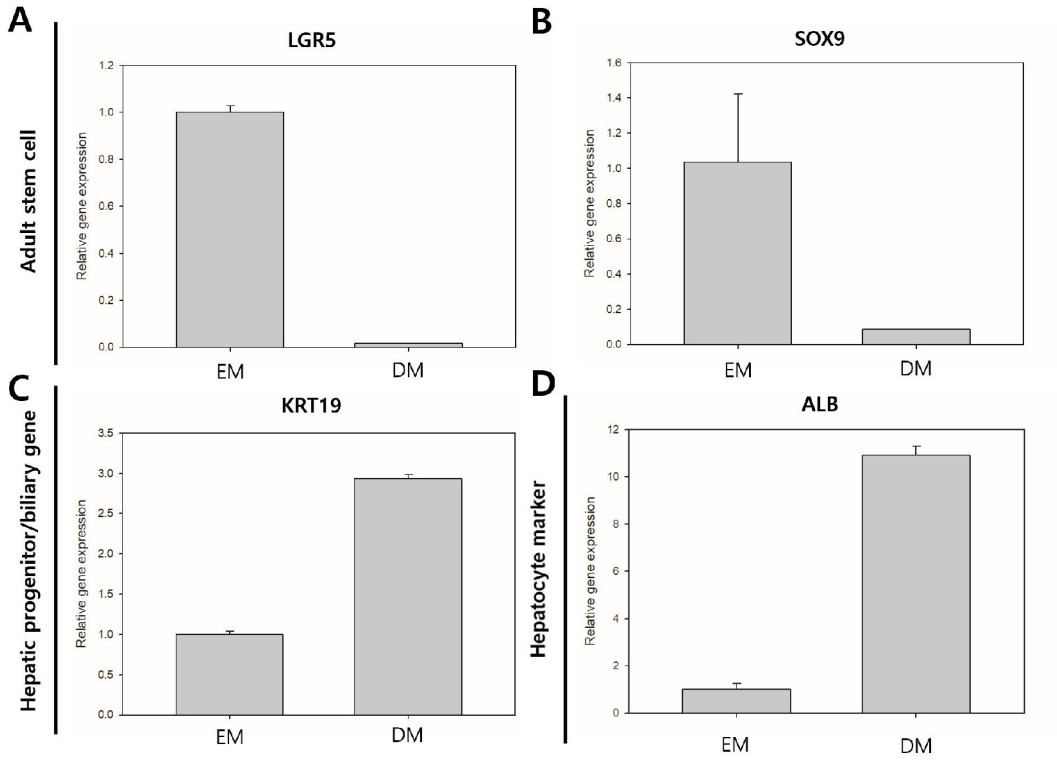

Figure 8. Relative gene expressions of mouse liver organoids cultured in the expansion medium and the differentiation medium. (A) LGR5; (B) SOX9; (C) KRT19; (D) ALB. Data are shown as mean ± standard error. EM = expansion medium, DM = differentiation medium.

2. Cell viability

ATP cell viability assay indicated that the viability of 10μM amiodarone-treated organoid group (94309.25 ± 3403.82 RLU) was significantly decreased when compared to that of control liver organoid group (141968.25 ± 1762.23 RLU) ($p<0.001$). At the same dose level of 10μM, the luminescence of cell viability was acetaminophen (129462.25 ± 1822.13 RLU) > amiodarone (94309.25 ± 3403.82 RLU) > tamoxifen (76076 ± 1257.61 RLU) = thioridazine (74622.25 ± 3839.29 RLU) (**Figure 9**). At the 20μM dose level, the luminescence of cell viability was tamoxifen (369 ± 33.36 RLU) = thioridazine (223.5 ± 5.97 RLU). The dose of tamoxifen and thioridazine were altered to 2.5 μM and 10 μM.

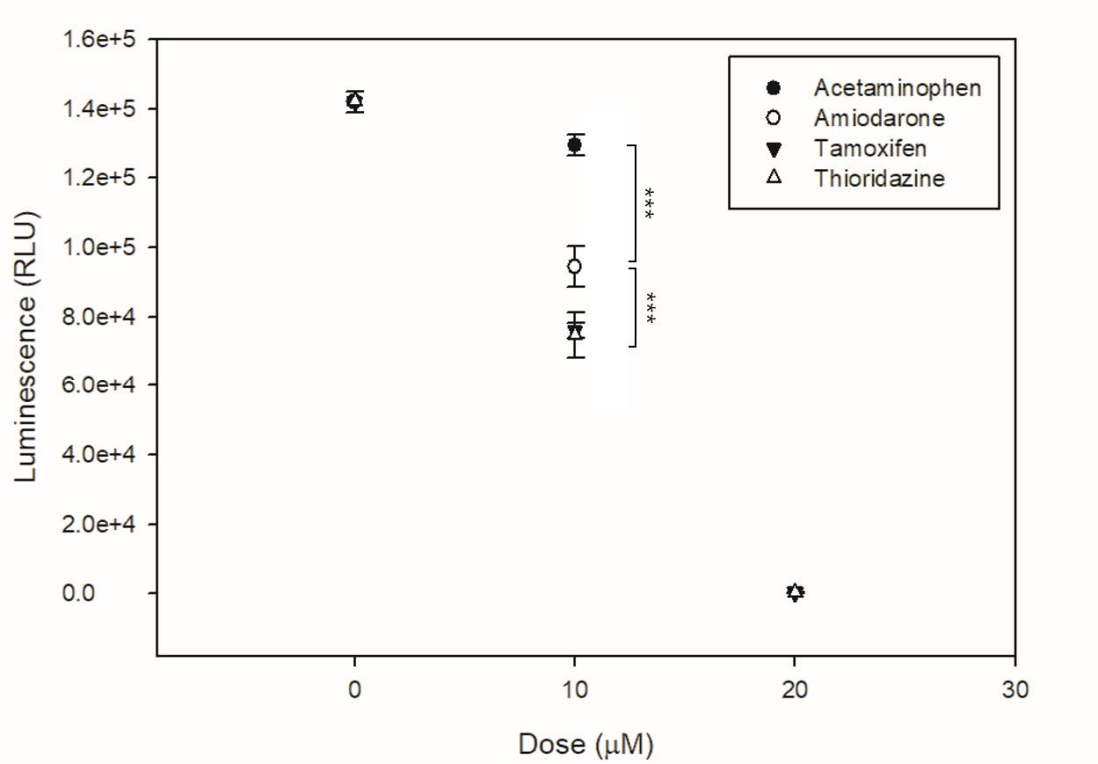

Figure 9. Comparison of ATP luminescence in control organoid group and treated organoid groups. Data are shown as mean ± standard error. *** $p < 0.001$.

Treatment	Dose	Mean	n	Standard error
Control	-	141968.2500	4	1762.23094
Acetaminophen	10	129462.2500	4	1822.12657
Amiodarone	10	94309.2500	4	3403.82266
Tamoxifen	10	76076.0000	4	1257.60586
Tamoxifen	20	369.0000	4	33.36165
Thioridazine	10	74622.2500	4	3839.28675
Thioridazine	20	233.5000	4	5.96518

Gene expression of ALB was associated with the ATP cell viability assay. The fold change of ALB in 10μM amiodarone-treated organoid group (0.275 ± 0.006 fold) was decreased when compared to that of control liver organoid group. At the same dose level of 10μM, the gene expression of ALB was amiodarone (0.275 ± 0.006 fold), acetaminophen (0.245 ± 0.047 fold), tamoxifen (0.082 ± 0.014 fold), and thioridazine (0.076 ± 0.022 fold) (**Figure 10**). At the 2.5μM dose level, the fold change of ALB was tamoxifen (0.131 ± 0.010 fold) and thioridazine (0.165 ± 0.018 fold).

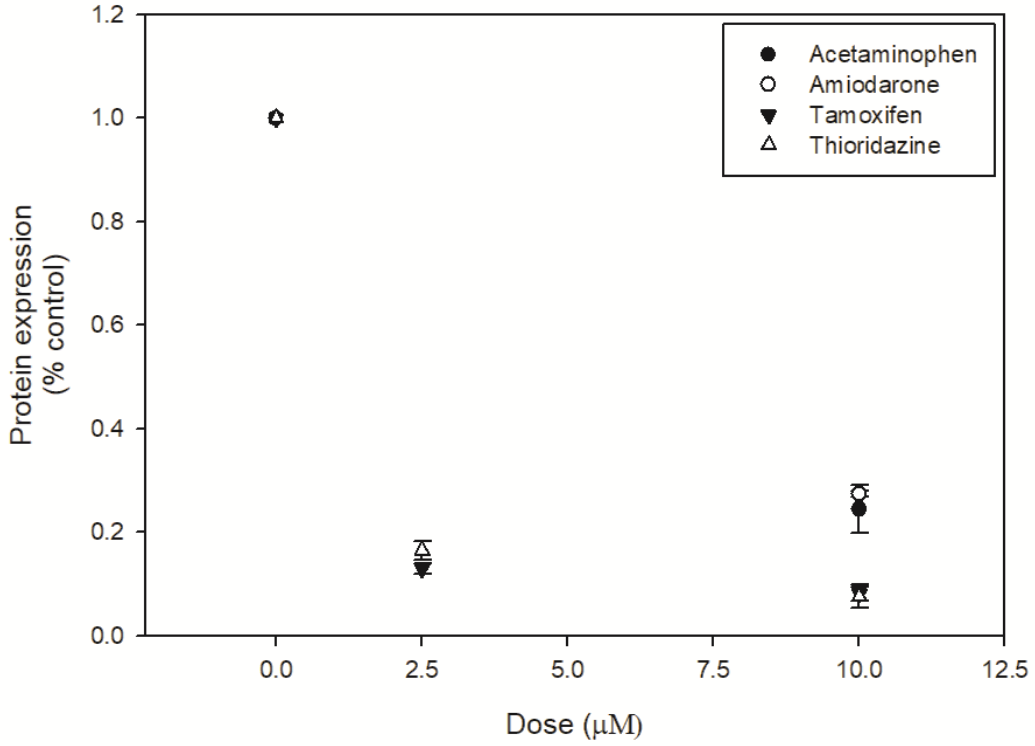

Figure 10. Relative gene expressions of CAD-treated mouse liver organoids. Data are shown as mean ± standard error.

3. DIPL in mouse liver 3D organoid

3.1. Histopathology

H&E staining demonstrated presence of fine vacuoles in cytoplasm of AMD-treated organoids and they were in the cytoplasm in the direction of the lumen (**Figure 11B**). These vacuoles were not seen in non-treated organoids (**Figure 11A**).

These fine vacuoles at cytoplasm of AMD-treated organoids were stained positive in immunohistochemical analyses (**Figure 12B**). The stained nuclear pattern was background effect, because this pattern was also found in non-treated organoids (**Figure 12A**).

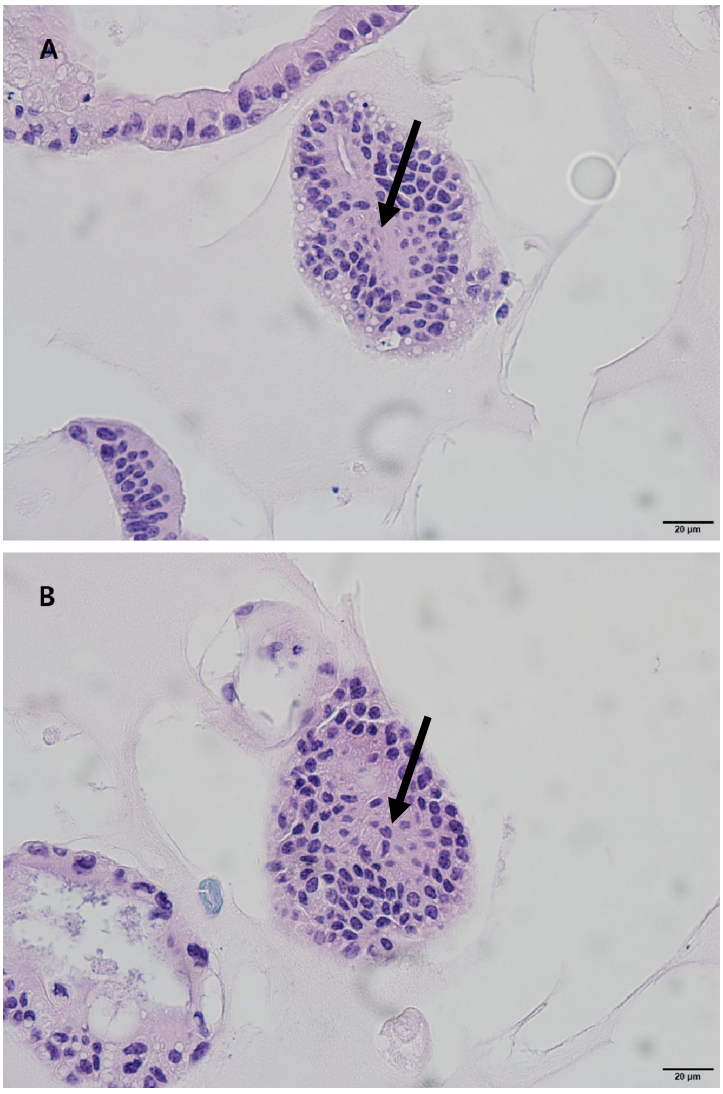

Figure 11. Representative mouse liver organoids with H&E staining. 400×. Scale bars = 20 µm. (A) Non-treated organoids, (B) AMD-treated organoids with fine vacuoles in cytoplasm.

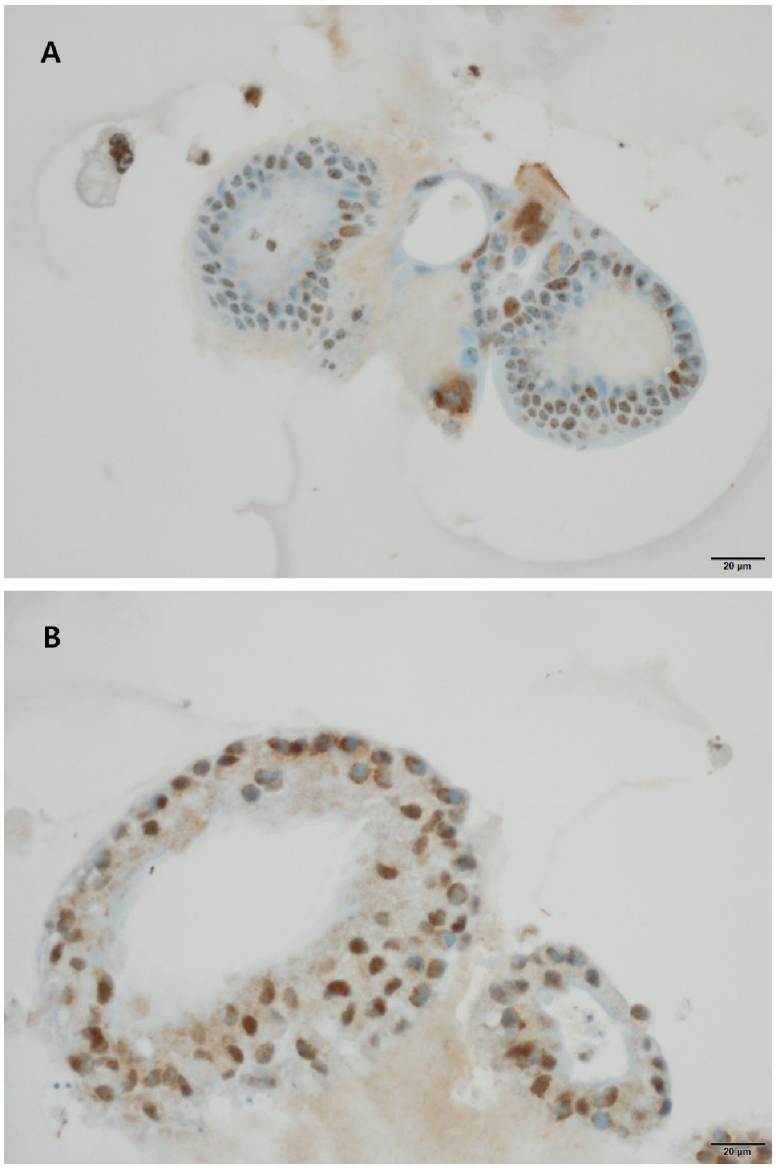

Figure 12. Immunohistochemistry for LAMP2. 400×. Scale bars = 20 μm. (A) Non-treated organoids, (B) AMD-treated organoids with fine vacuoles in cytoplasm.

3.2. Electron microscopy

Whereas multilamellar bodies, a hallmark of DIPL, were not seen in non-treated organoids (**Figure 13A**), the remarkable aggregations of multilamellar bodies were identified in cytoplasm of the almost every amiodarone-treated organoids by transmission electron microscopic examination (**Figure 13B, C**). The multilamellar bodies had a typical appearance, which was consistent with the previously reported forms.

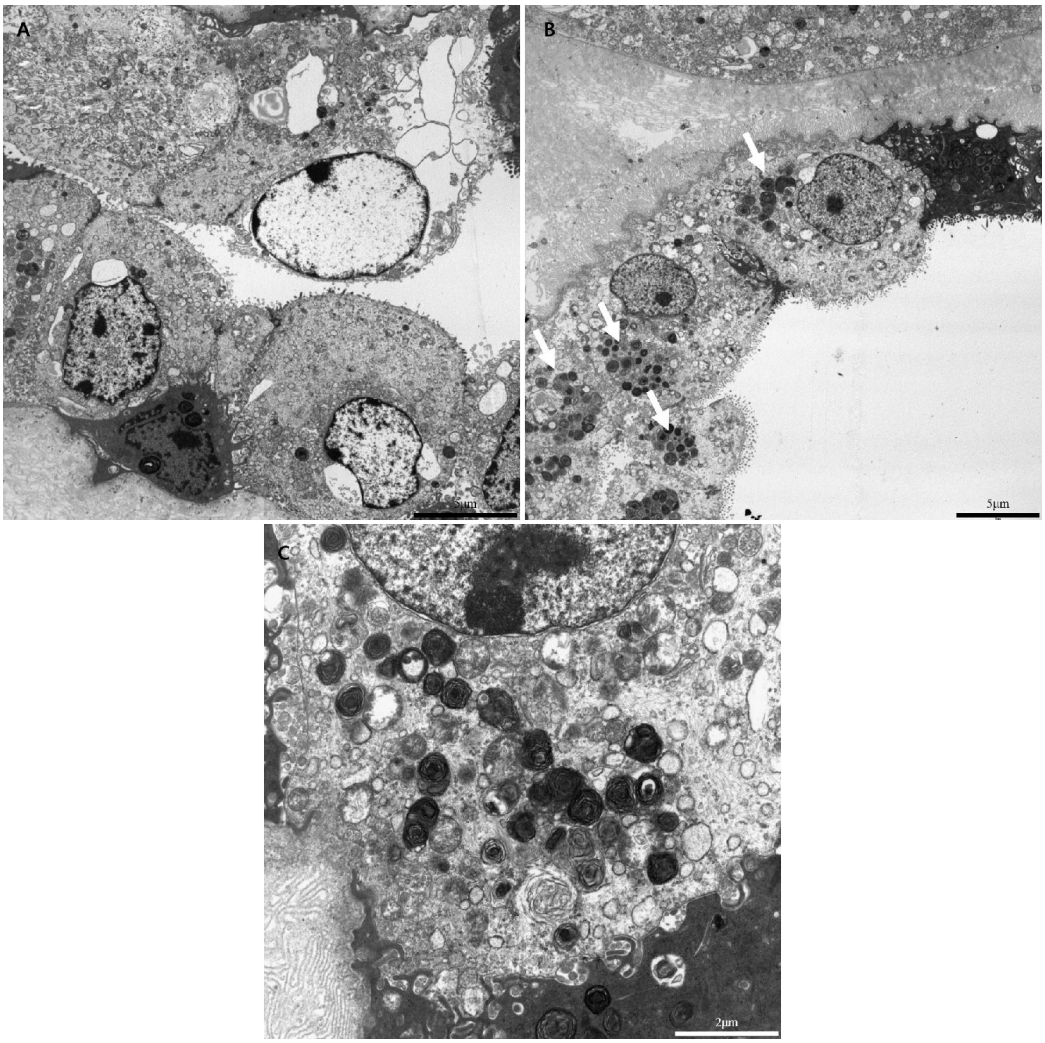

Figure 13. Representative electron microscopy images of the mouse liver organoids. (A) Non-treated mouse liver organoids. 4,000×. Scale bar = 5μm. (B) 10μM amiodarone-treated mouse liver organoids for 72h. The arrows show intracytoplasmic multilamellar bodies. 3,000×. Scale bar = 5μm. (C) Higher magnification of the multilamellar bodies. 10,000×. Scale bar = 2μm.

3.3. Gene expression of ASAH1

Relative ASAH1 level of amiodarone-treated organoids was about 1.45 times higher than the level of non-treated organoids. And the mRNA level of the 10 μM tamoxifen-treated group was increased about 2.27 times compared with the level of the 2.5 μM tamoxifen-treated group. Therefore, dose dependency was found in two tamoxifen-treated groups. There was no difference between two thioridazine-treated groups.

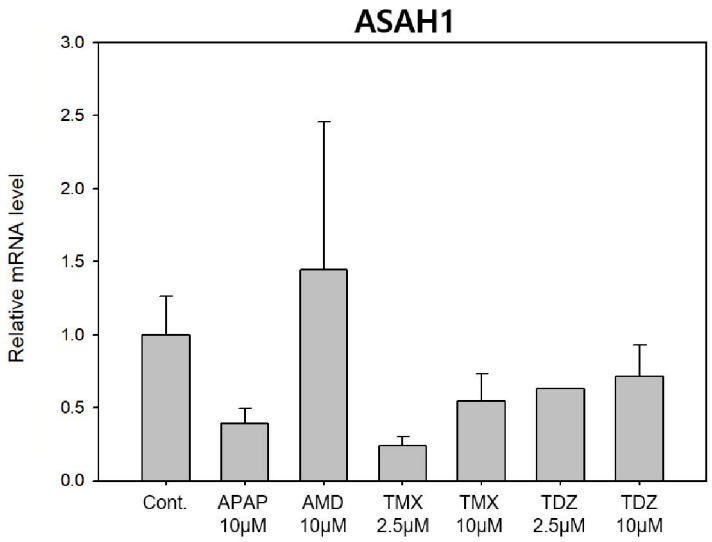

Figure 14. Relative ASAH1 expressions of CAD-treated mouse liver organoids. Data are shown as mean ± standard error

Treatment	Dose	Mean	Standard error
Control	-	1	0.264988
Acetaminophen	10	0.391259	0.101239
Amiodarone	10	1.446392	1.011548
Tamoxifen	2.5	0.239973	0.064512
Tamoxifen	10	0.54455	0.184765
Thioridazine	2.5	0.632141	-
Thioridazine	10	0.714579	0.215094

4. DIPL in *in vivo* mouse liver

Hepatocytes with foamy cytoplasm were identified at peri-central veins of amiodarone-treated mouse (**Figure 15B**) and were not seen in vehicle-treated group (**Figure 15A**). This lesion was found only in amiodarone-treated group.

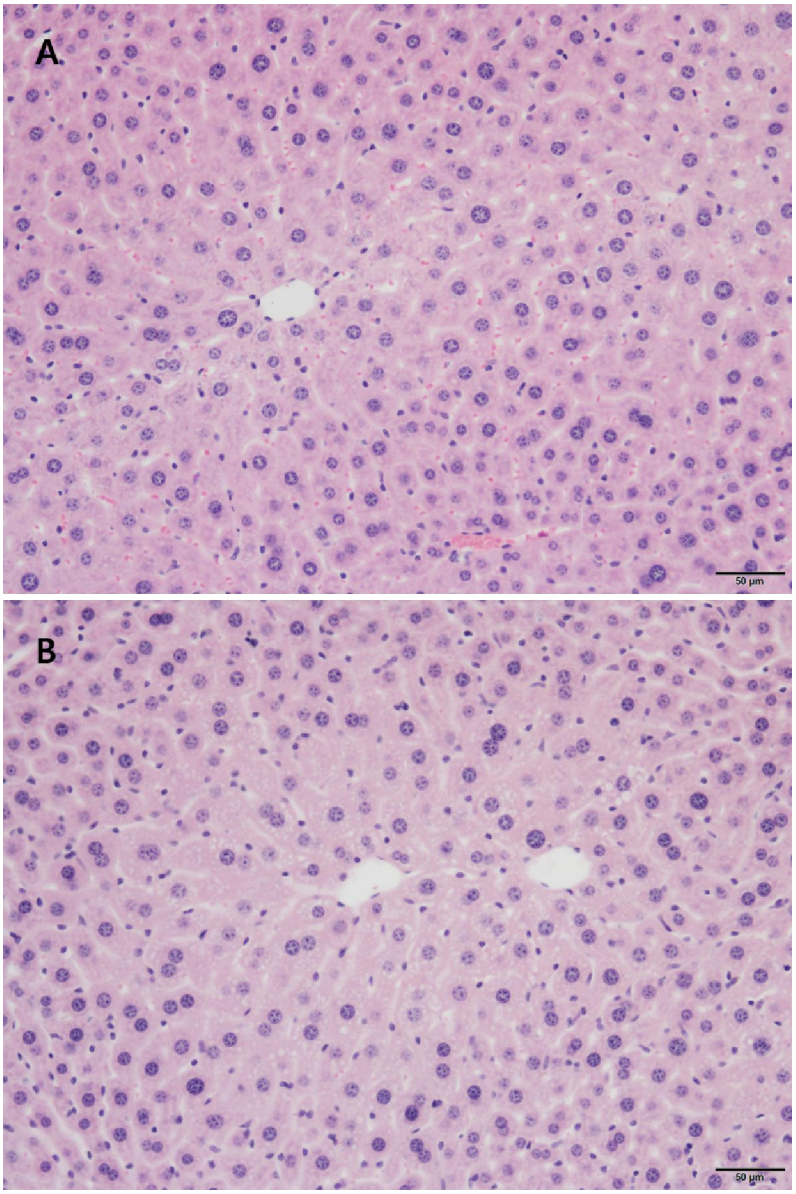

Figure 15. Representative mouse liver with H&E staining. 200× (A) Vehicle-treated mouse liver. 200×. Scale bar = 50µm. (B) Amiodarone-treated mouse liver. 200×. Scale bar = 50µm.

Discussion

The purpose of this study was to estimate whether the phenomena of amiodarone-induced phospholipidosis in mouse liver organoids were identical with those of *in vivo* mouse toxicity studies. Before evaluating induction of DIPL in our organoids, we needed to make sure that our model had similar structures or functions of liver. Morphological evaluation showed that our model was differentiated into uniformly polygonal cells which had round to oval nucleus; one nucleolus; and abundant cytoplasm, which were similar with *in vivo* hepatocytes. And the organoids showed a notable lower expression of LGR5 (0.016 fold) and SOX9 (0.085 fold), adult stem cell genes, a higher expression of KRT19 (2.928 fold), hepatic progenitor/biliary gene, and of ALB (10.907 fold), early hepatocyte gene. These morphological evaluation and results of gene expression suggested that our model was identical with those of 'hepatocyte like cells' or 'intermediate hepatocyte' in the previous studies (Huch et al., 2013; Kuijk et al., 2016).

Previous *in vitro* studies showed that detection of the multilamellar bodies using the transmission electron microscopy or other *in vitro* assays could be used for detection and screening of potential phospholipogenic compounds in conventional cultures (Bhandari et al., 2008; Glock, Muehlbacher, Hurtig, Tripal, & Kornhuber, 2016; Teresa Donato & Jose Gomez-Lechon, 2012). Interestingly, the transmission electron microscopy examination showed the intracytoplasmic aggregations of the multilamellar bodies, a hallmark of DIPL, in our organoid model. The multilamellar bodies had a typical appearance, which was consistent with the previously reported forms (Poucell et al., 1984).

In addition to the identification of multilamellar bodies through transmission electron microscopy, microscopic examination with H&E staining demonstrated presence of fine vacuoles in cytoplasm of AMD-treated organoids and they were in the cytoplasm in the direction of the lumen. In immunohistochemical analyses, LAMP-2 stained positively and showed cytoplasmic patterns in AMD-treated organoids. These histopathological results were not observed in the vehicle group or the APAP-treated group. Consistent with what was observed in the organoids, the fine vacuoles in hepatocellular cytoplasm were identified at peri-central veins of AMD-treated *in vivo* liver.

Relative ASAH1 expression level of AMD-treated organoids was higher than the level of non-treated organoids (1.45-fold). It was known that ASAH1 gene was involved in the

induction of DIPL in *in vitro* systems such as HepG2 and rat primary hepatocytes (Fujimura, Murakami, Kurabe, & Toriumi, 2009; Sawada, Takami, & Asahi, 2004). Our results showed that mouse liver 3D organoid model could be able to monitor the induction of DIPL.

In conclusion, our findings suggest that mouse liver organoids can reflect well the expected or well-known outcomes in DIPL-induced *in vivo* mouse and can support further researches for predicting the DIPL in liver organoids.

References

Anderson, N., & Borlak, J. (2006). Drug□induced phospholipidosis. *FEBS letters, 580*(23), 5533-5540.

Bell, C. C., Lauschke, V. M., Vorrink, S. U., Palmgren, H., Duffin, R., Andersson, T. B., & Ingelman-Sundberg, M. (2017). Transcriptional, Functional, and Mechanistic Comparisons of Stem Cell–Derived Hepatocytes, HepaRG Cells, and Three-Dimensional Human Hepatocyte Spheroids as Predictive In Vitro Systems for Drug-Induced Liver Injury. *Drug metabolism and disposition, 45*(4), 419-429.

Bhandari, N., Figueroa, D. J., Lawrence, J. W., & Gerhold, D. L. (2008). Phospholipidosis assay in HepG2 cells and rat or rhesus hepatocytes using phospholipid probe NBD-PE. *Assay and drug development technologies, 6*(3), 407-419.

Broutier, L., Andersson-Rolf, A., Hindley, C. J., Boj, S. F., Clevers, H., Koo, B.-K., & Huch, M. (2016). Culture and establishment of self-renewing human and mouse adult liver and pancreas 3D organoids and their genetic manipulation. *Nature protocols, 11*(9), 1724.

Chatman, L. A., Morton, D., Johnson, T. O., & Anway, S. D. (2009). A strategy for risk management of drug-induced phospholipidosis. *Toxicol Pathol, 37*(7), 997-1005.

Cherblanc, F., Chapman-Rothe, N., Brown, R., & Fuchter, M. (2012). Current limitations and future opportunities for epigenetic therapies. *Future medicinal chemistry, 4*(4), 425-446.

David, S., & Hamilton, J. P. (2010). Drug-induced liver injury. *US gastroenterology & hepatology review, 6*, 73.

Edmondson, R., Broglie, J. J., Adcock, A. F., & Yang, L. (2014). Three-dimensional cell culture systems and their applications in drug discovery and cell-based biosensors. *Assay and drug development technologies, 12*(4), 207-218.

Fatehullah, A., Tan, S. H., & Barker, N. (2016). Organoids as an in vitro model of human development and disease. *Nature cell biology, 18*(3), 246.

Fujimura, H., Murakami, N., Kurabe, M., & Toriumi, W. (2009). In vitro assay for

drug□induced hepatosteatosis using rat primary hepatocytes, a fluorescent lipid analog and gene expression analysis. *Journal of Applied Toxicology, 29*(4), 356-363.

Funk, C., & Roth, A. (2017). Current limitations and future opportunities for prediction of DILI from in vitro. *Archives of toxicology, 91*(1), 131-142.

Glock, M., Muehlbacher, M., Hurtig, H., Tripal, P., & Kornhuber, J. (2016). Drug-induced phospholipidosis caused by combinations of common drugs in vitro. *Toxicology in Vitro, 35*, 139-148.

Godoy, P., Hewitt, N. J., Albrecht, U., Andersen, M. E., Ansari, N., Bhattacharya, S., . . . Böttger, J. (2013). Recent advances in 2D and 3D in vitro systems using primary hepatocytes, alternative hepatocyte sources and non-parenchymal liver cells and their use in investigating mechanisms of hepatotoxicity, cell signaling and ADME. *Archives of toxicology, 87*(8), 1315.

Halliwell, W. H. (1997). Cationic amphiphilic drug-induced phospholipidosis. *Toxicol Pathol, 25*(1), 53-60.

Horn, J., Jensen, C., White, S., Laska, D., Novilla, M., Giera, D., & Hoover, D. (1996). In vitro and in vivo ultrastructural changes induced by macrolide antibiotic LY281389. *Toxicological sciences, 32*(2), 205-216.

Huch, M., Dorrell, C., Boj, S. F., Van Es, J. H., Li, V. S., Van De Wetering, M., . . . Finegold, M. J. (2013). In vitro expansion of single Lgr5+ liver stem cells induced by Wnt-driven regeneration. *Nature, 494*(7436), 247.

Huch, M., Gehart, H., Van Boxtel, R., Hamer, K., Blokzijl, F., Verstegen, M. M., . . . de Ligt, J. (2015). Long-term culture of genome-stable bipotent stem cells from adult human liver. *Cell, 160*(1), 299-312.

Kodavanti, U. P., & Mehendale, H. M. (1990). Cationic amphiphilic drugs and phospholipid storage disorder. *Pharmacological Reviews, 42*(4), 327-354.

Kuijk, E. W., Rasmussen, S., Blokzijl, F., Huch, M., Gehart, H., Toonen, P., . . . Cuppen, E. (2016). Generation and characterization of rat liver stem cell lines and their engraftment in a rat model of liver failure. *Scientific reports, 6*, 22154.

Kullak-Ublick, G. A., Andrade, R. J., Merz, M., End, P., Benesic, A., Gerbes, A. L., & Aithal, G. P. (2017). Drug-induced liver injury: recent advances in diagnosis and risk assessment. *Gut, 66*(6), 1154-1164.

Leite, S. B., Wilk-Zasadna, I., Zaldivar, J. M., Airola, E., Reis-Fernandes, M. A., Mennecozzi, M., . . . Alves, P. M. (2012). Three-dimensional HepaRG model as an attractive tool for toxicity testing. *Toxicological sciences, 130*(1), 106-116.

Nantasanti, S., Spee, B., Kruitwagen, H. S., Chen, C., Geijsen, N., Oosterhoff, L. A., . . . Wubbolts, R. W. (2015). Disease modeling and gene therapy of copper storage disease in canine hepatic organoids. *Stem cell reports, 5*(5), 895-907.

Nioi, P., Perry, B. K., Wang, E.-J., Gu, Y.-Z., & Snyder, R. D. (2007). In vitro detection of drug-induced phospholipidosis using gene expression and fluorescent phospholipid–based methodologies. *Toxicological sciences, 99*(1), 162-173.

Nonoyama, T., & Fukuda, R. (2008). Drug-induced phospholipidosis-pathological aspects and its prediction. *Journal of toxicologic pathology, 21*(1), 9-24.

Otieno, M. A., Snoeys, J., Lam, W., Ghosh, A., Player, M. R., Pocai, A., . . . Singh, B. (2017). Fasiglifam (TAK-875): mechanistic investigation and retrospective identification of hazards for drug induced liver injury. *Toxicological sciences, 163*(2), 374-384.

Poucell, S., Ireton, J., Valencia-Mayoral, P., Downar, E., Larratt, L., Patterson, J., . . . Phillips, M. (1984). Amiodarone-associated phospholipidosis and fibrosis of the liver. Light, immunohistochemical, and electron microscopic studies. *Gastroenterology, 86*(5 Pt 1), 926-936.

Reasor, M. J., Hastings, K. L., & Ulrich, R. G. (2006). Drug-induced phospholipidosis: issues and future directions. *Expert opinion on drug safety, 5*(4), 567-583.

Sawada, H., Takami, K., & Asahi, S. (2004). A toxicogenomic approach to drug-induced phospholipidosis: analysis of its induction mechanism and establishment of a novel in vitro screening system. *Toxicological sciences,*

83(2), 282-292.

Schyschka, L., Sánchez, J. M., Wang, Z., Burkhardt, B., Müller-Vieira, U., Zeilinger, K., . . . Nussler, A. (2013). Hepatic 3D cultures but not 2D cultures preserve specific transporter activity for acetaminophen-induced hepatotoxicity. *Archives of toxicology, 87*(8), 1581-1593.

Seydel, J. K., & Wassermann, O. (1976). NMR-studies on the molecular basis of drug-induced phospholipidosis—II. Interaction between several amphiphilic drugs and phospholipids. *Biochemical pharmacology, 25*(21), 2357-2364.

Si-Tayeb, K., Lemaigre, F. P., & Duncan, S. A. (2010). Organogenesis and development of the liver. *Developmental cell, 18*(2), 175-189.

Somani, P., Bandyopadhyay, S., Klaunig, J. E., & Gross, S. A. (1990). Amiodarone□and desethylamiodarone□induced myelinoid inclusion bodies and toxicity cultured rat hepatocytes. *Hepatology, 11*(1), 81-92.

Stevens, J. L., & Baker, T. K. (2009). The future of drug safety testing: expanding the view and narrowing the focus. *Drug discovery today, 14*(3-4), 162-167.

Takahashi, Y., Hori, Y., Yamamoto, T., Urashima, T., Ohara, Y., & Tanaka, H. (2015). 3D spheroid cultures improve the metabolic gene expression profiles of HepaRG cells. *Bioscience reports, 35*(3), e00208.

Teresa Donato, M., & Jose Gomez-Lechon, M. (2012). Drug-induced liver steatosis and phospholipidosis: cell-based assays for early screening of drug candidates. *Current drug metabolism, 13*(8), 1160-1173.

Summary in Korean

약물에 의해 유도된 간 손상은 신약 승인 철회 및 시판 중인 약물의 사용 제한 등의 주요 요인이다. 최근 약물 유도 간 손상을 효율적으로 예측하기 위해, 다양한 간세포 모델에 대한 연구가 활발히 진행되고 있다. 간 오가노이드는 3 차원에서 일차 간세포 또는 간 줄기 세포를 배양하는 시험관 내 시스템으로, 2 차원 모델이나 샌드위치 배양법과 같은 기존의 시험관 내 배양 모델에 비해 비교적 장기간 동안 생체내 간과 생리적으로 유사하다는 장점이 알려져 있어 초기 약물 개발 및 독성학 분야에서 유용한 모델로 간주된다. 인지질증은 약물 유도 간 손상의 일환으로, 영향 받은 세포의 세포질 내에 인지질-약물 복합체가 축적되어 관찰되는 일종의 지질 저장 장애 질환이다. 간은 이 인지질증이 초기 독성시험에서 흔히 관찰되는 장기 중 하나로, 규제 기관에서는 이 인지질증에 대한 독성 시험시, 설치류 및 비설치류를 이용한 2 주 시험을 수행할 것을 권고하고 있다. 본 연구의 목적은 인지질증이 유도된 간 오가노이드와 생체 내에서의 결과를 비교하는 것이며, 본 연구는 가장 초기 독성 시험에서 이용되는 마우스를 동물종으로 선택하여 마우스 간 3 차원 오가노이드 및 생체 내 마우스에서 수행되었다. 이를 위해 첫번째, 본 실험실에서 제작한 마우스 간 3 차원 오가노이드의 특성화 평가를 수행하였고, 두번째, 대표적인 양친매성 물질에 의해 마우스 간 3 차원 오가노이드에 인지질증이 유도되었는지 확인하였다. 마지막으로, 인지질증이 유도된 마우스 간 3 차원 오가노이드와 생체 내 마우스에서의 결과를 비교하였다. 오가노이드의 특성화 평가 결과, 간 오가노이드는 관 세포보다 간세포에 유사한 구조를 가진 것을 확인하였으며, 초기 단계 간세포와 유사한 단백질 발현을 나타내었다. 이후 약물 투여시 세포 생존력이 유의하게 감소하였으며, 투과전자현미경을 통해 인지질증의 확진 지표인 세포내 층판소체를 발견함으로써 오가노이드에서 인지질증이 유도된 것을 확인하였다. 본 연구 결과는 인지질증이 유도된 마우스 간 오가노이드에서 생체 내 마우스에서 예상되거나 잘 알려진 결과를 반영할 수 있으며 간 오가노이드를 이용한 약물 유도 인지질증 예측에 대한 추가 연구를 뒷받침 할 수 있음을 시사한다.